Supplementary Materials

A. Endurance measurements

During endurance testing over $3 \cdot 10^6$ switching cycles, the write error rate for switching between the extreme resistive states (HRS and LRS) could reach up to 0.000013% in individual cases. For multilevel state programming, the write error rate was found to be less than 1%, confirming both the reliability of the devices and the consistency of their switching parameters across the array. To further assess the reliability under repeated programming, the devices were cycled more than 25000 times, demonstrating stable resistive switching without performance degradation.

Moreover, the memristor demonstrates high endurance over a wide temperature range (**Figure S1**, **Table S1**).

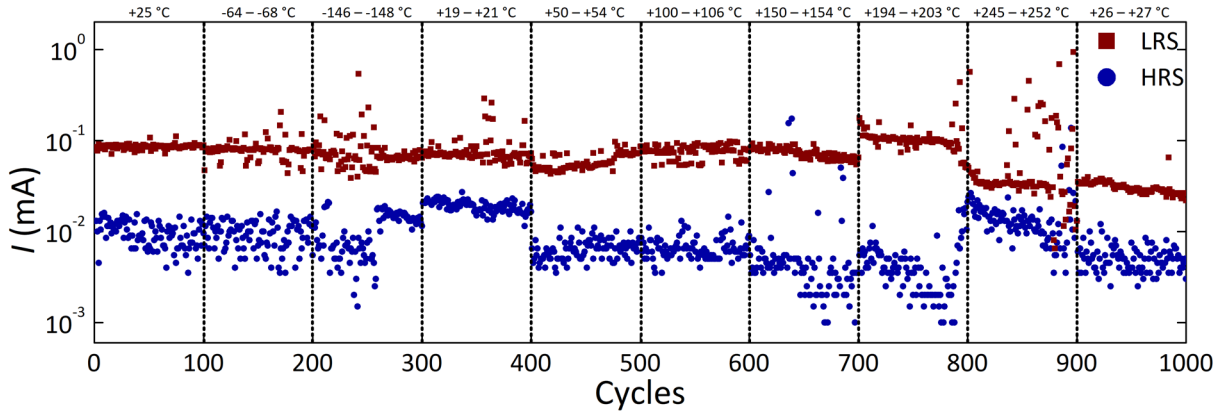
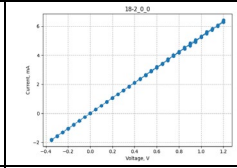
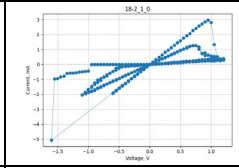
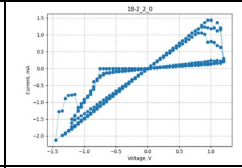
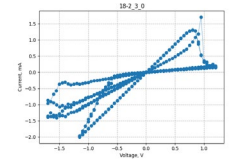
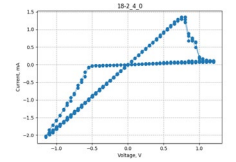
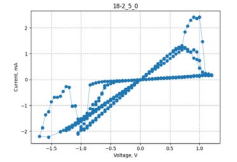
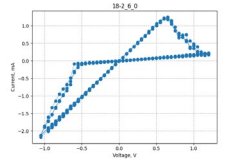
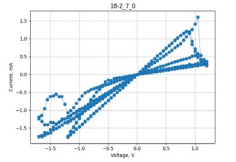
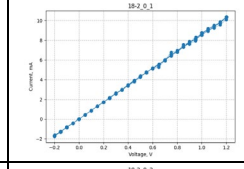
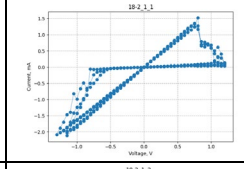
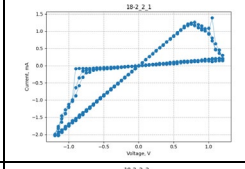
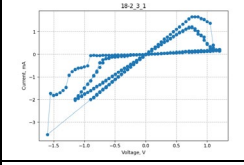
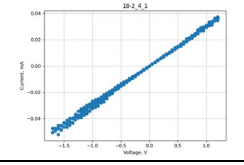
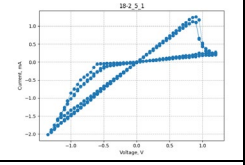
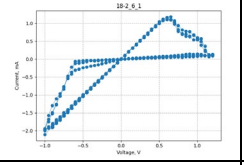
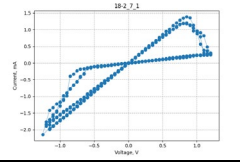
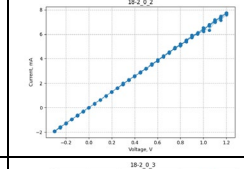
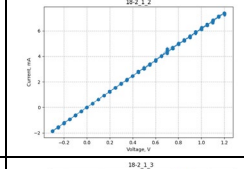
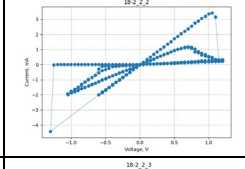
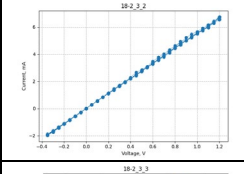
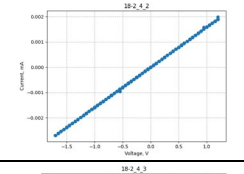
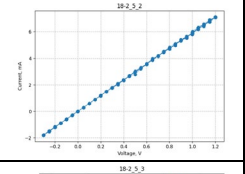
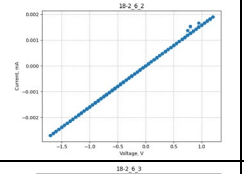
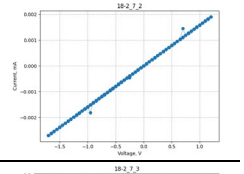
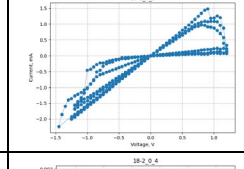
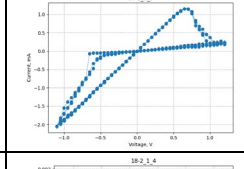
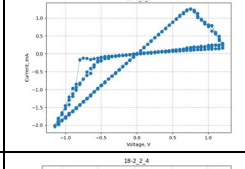
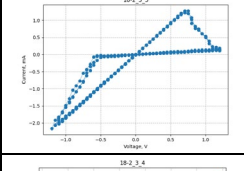
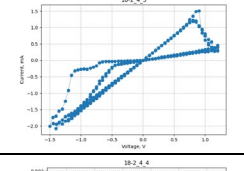
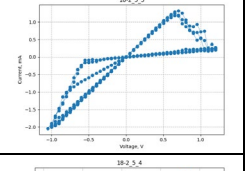
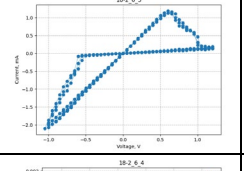
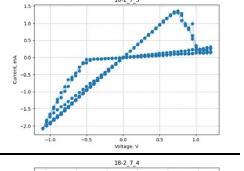
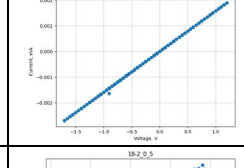
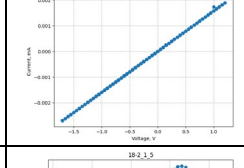
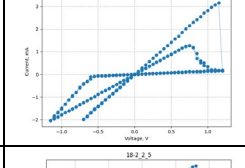
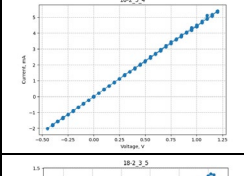
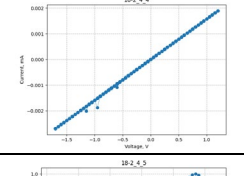
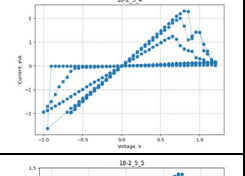
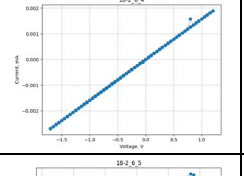
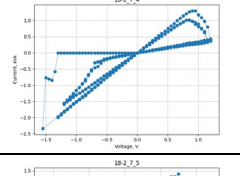


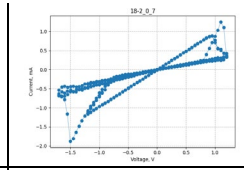
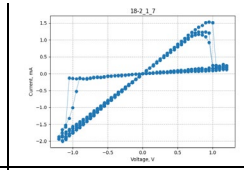
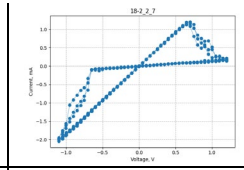
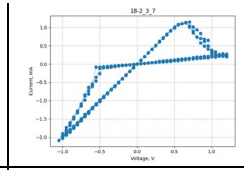
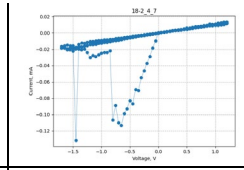
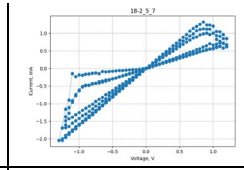
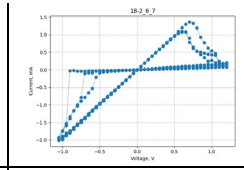
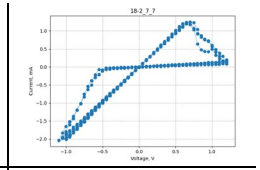
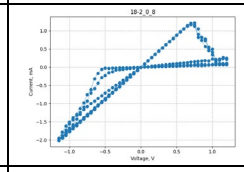
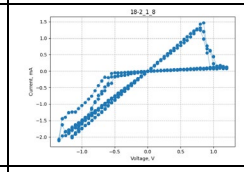
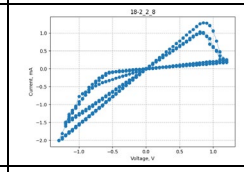
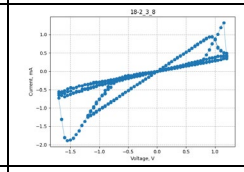
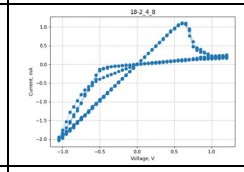
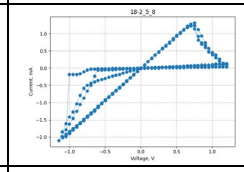
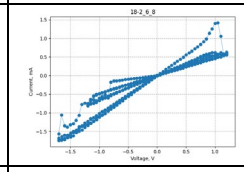
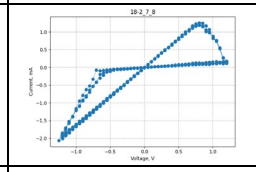
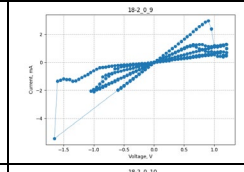
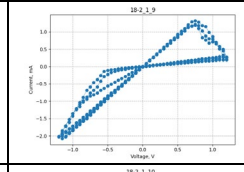
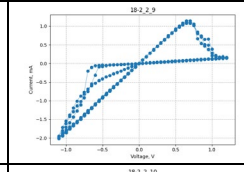
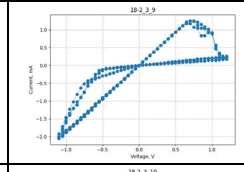
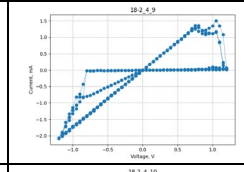
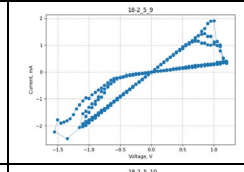
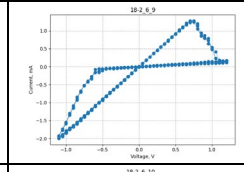
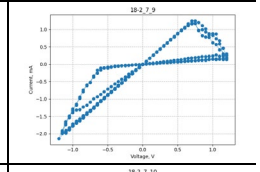
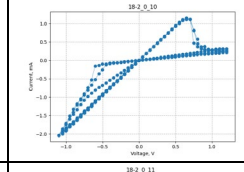
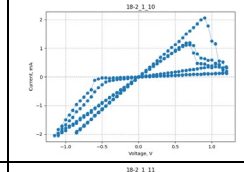
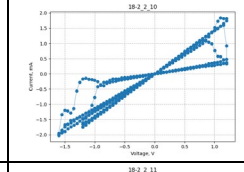
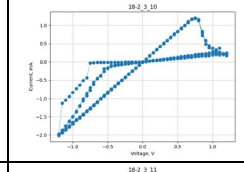
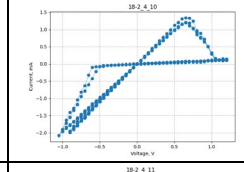
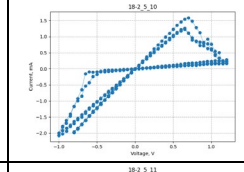
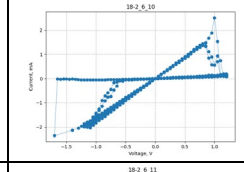
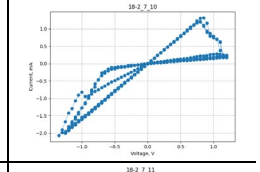
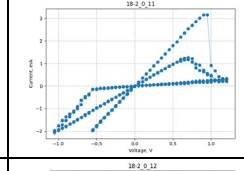
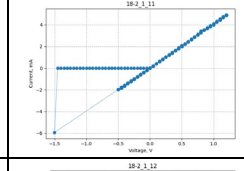
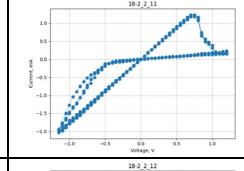
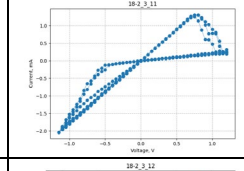
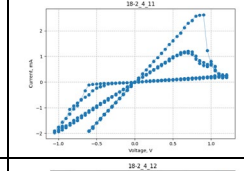
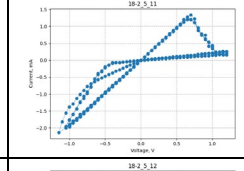
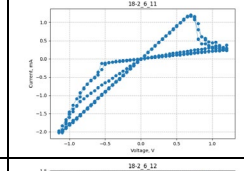
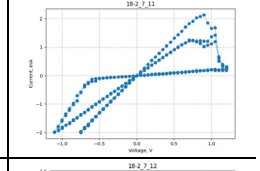
Figure S1. Temperature dependence of endurance for ZrO_2(Y)-based memristive devices.

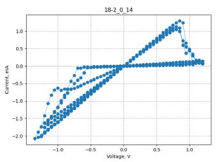
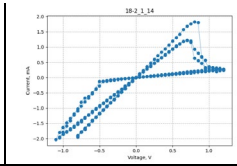
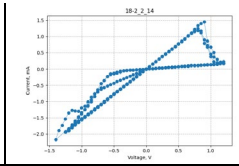
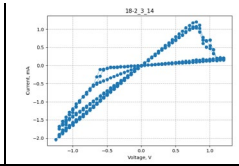
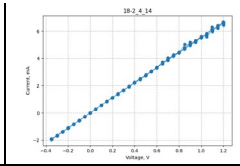
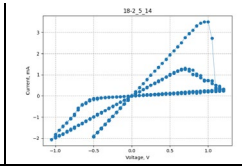
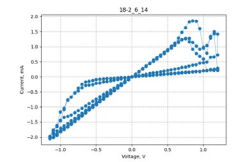
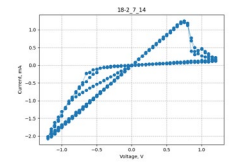
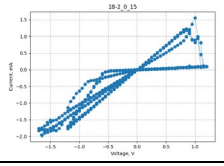
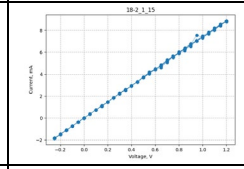
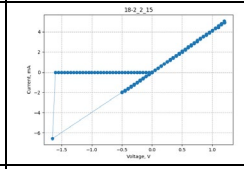
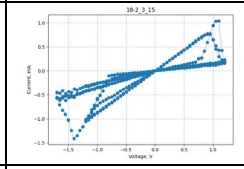
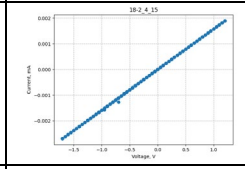
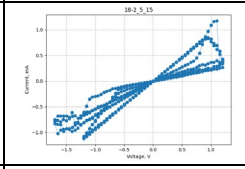
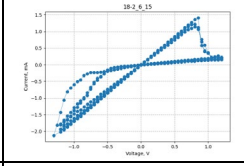
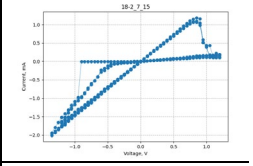
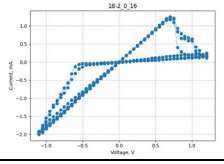
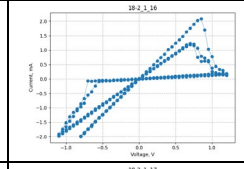
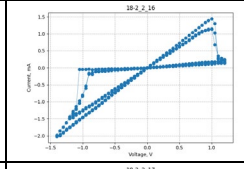
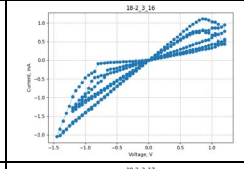
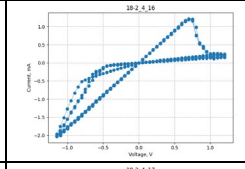
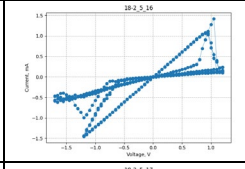
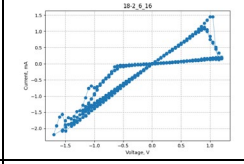
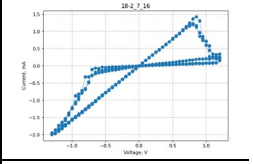
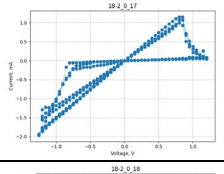
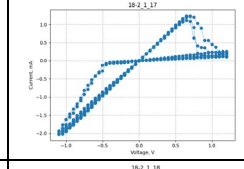
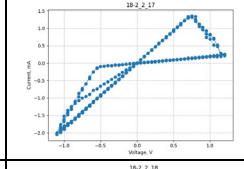
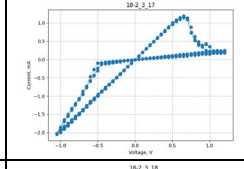
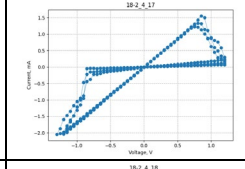
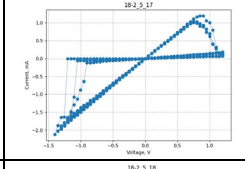
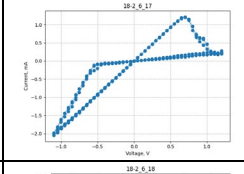
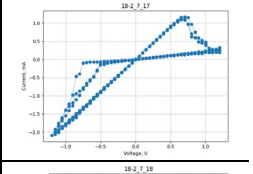
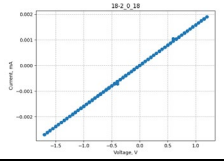
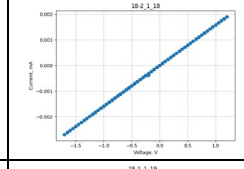
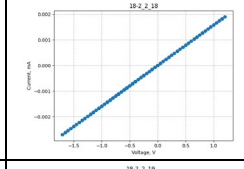
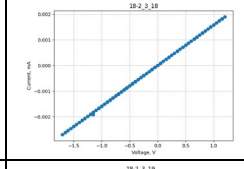
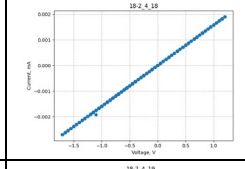
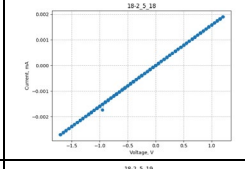
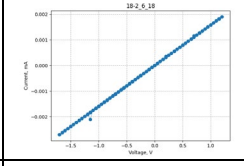
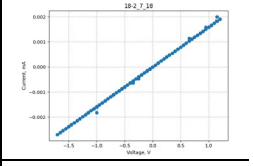
Table S1. Temperature-dependent statistical analysis of currents in LRS and HRS: average values (μ), standard deviations (σ), and coefficients of variation ($c = \sigma/\mu$).

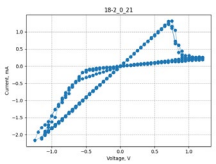
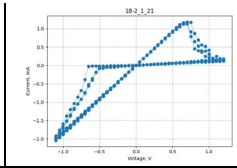
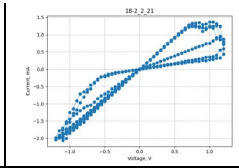
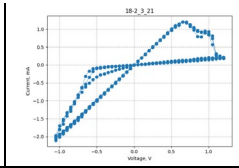
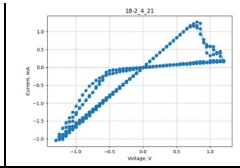
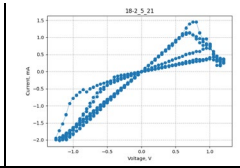
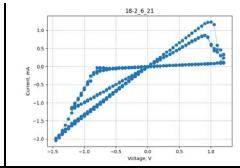
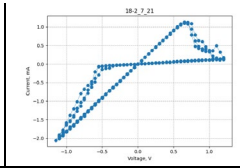
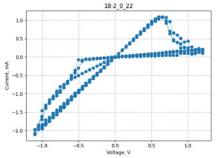
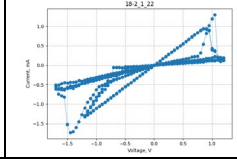
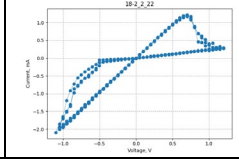
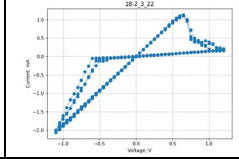
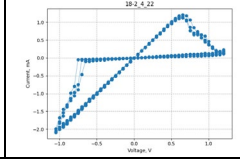
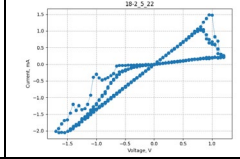
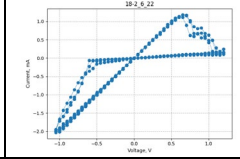
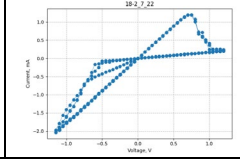
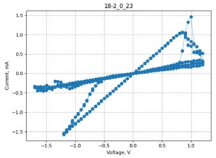
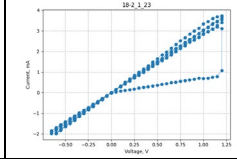
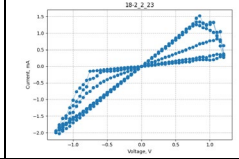
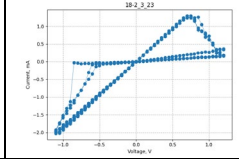
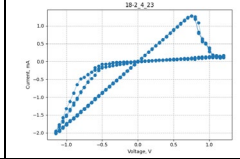
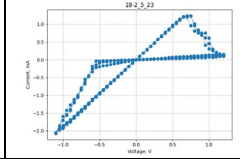
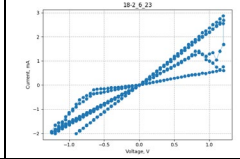
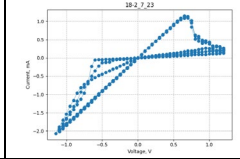
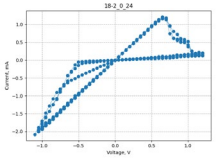
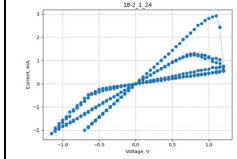
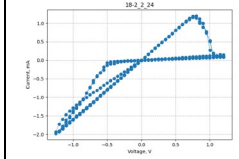
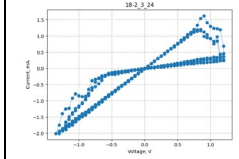
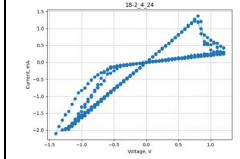
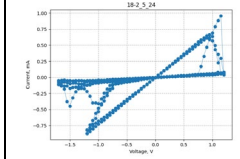
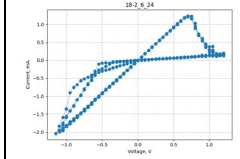
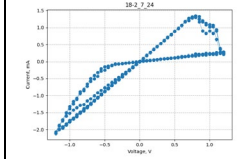
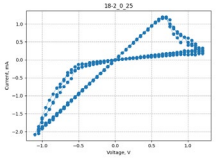
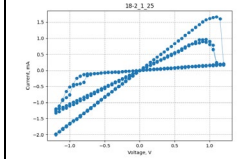
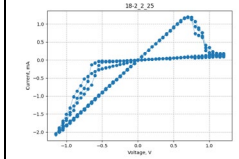
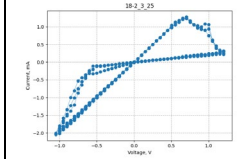
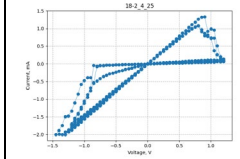
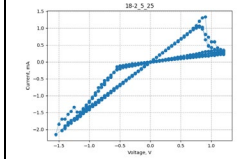
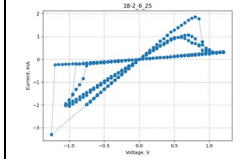
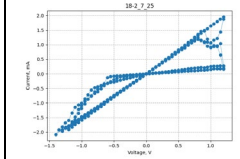
***T*, °C**	**LRS**			**HRS**			μ_{LRS}/μ_{HRS}
	***μ*, μA**	***σ*, μA**	***c*, %**	***μ*, μA**	***σ*, μA**	***c*, %**	
+25	86	5.3	6.2	9.7	3.0	31	8.9
-64 – -68	80	20	25	9.5	3.3	35	8.4
-146 – -148	79	55	70	11	5.1	49	7.2
+19 – +21	80	36	45	19	2.7	14	4.2
+50 – +54	59	12	20	6.5	1.7	26	9.1
+100 – +106	76	12	16	6.7	2.0	30	11.3
+150 – +154	73	9.5	13	9.3	24	258	7.8
+194 – +203	106	42	40	4.7	3.7	79	23
+245 – +252	80	137	171	16	16	100	5.0
+26 – +27	31	5.2	17	5.2	1.7	33	6.0

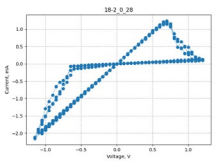
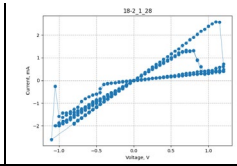
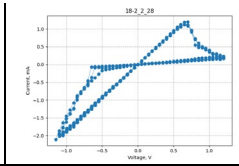
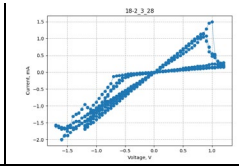
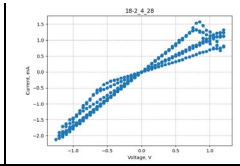
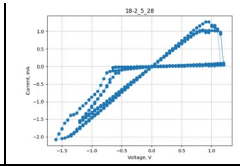
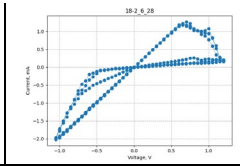
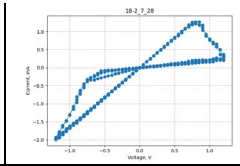
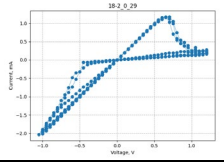
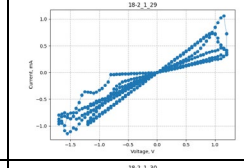
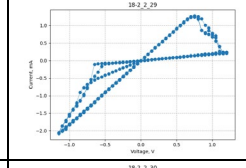
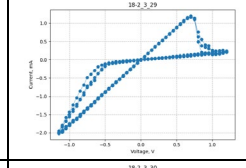
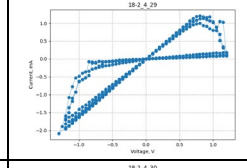
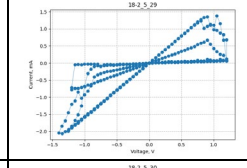
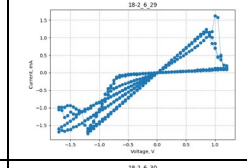
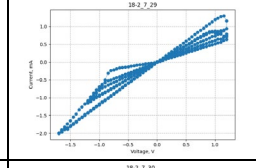
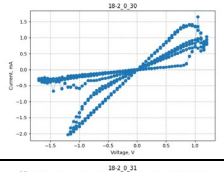
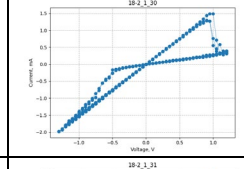
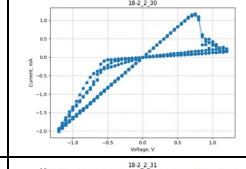
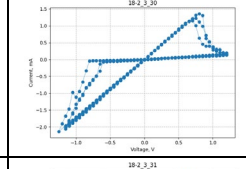
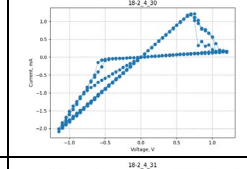
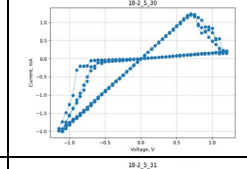
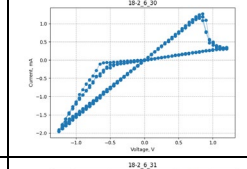
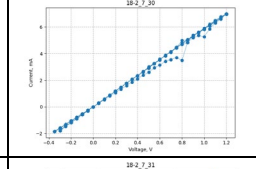
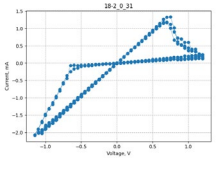
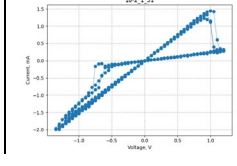
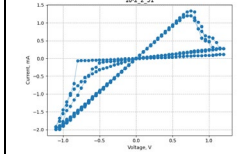
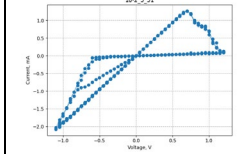
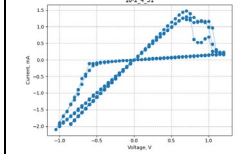
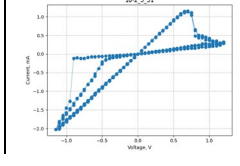
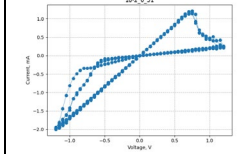
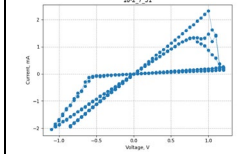
Table S2. *I–V* curve maps of all 256 ZrO_2(Y)-based memristive devices in the 32×8 1T1R crossbar array.

	WL0	WL1	WL2	WL3	WL4	WL5	WL6	WL7
BL0								
BL1								
BL2								
BL3								
BL4								
BL5								
BL6								

BL7								
BL8								
BL9								
BL10								
BL11								
BL12								
BL13								

BL14								
BL15								
BL16								
BL17								
BL18								
BL19								
BL20								

BL21								
BL22								
BL23								
BL24								
BL25								
BL26								
BL27								

BL28								
BL29								
BL30								
BL31								

The *I–V* curves of all 256 memristive devices are presented as a matrix in **Table S2**. For each device, the measurement sequence includes an initial SET (or electroforming) cycle, followed by a RESET cycle, and then three subsequent *I–V* curves. These measurements were performed prior to any training or tuning of the devices, thus reflecting the as-fabricated state of the crossbar array. The curves exhibit a consistent shape across the entire 32×8 array under the same measurement protocol with absolute voltage values in the 1–1.5 V range, confirming the good uniformity and low device-to-device variation of the fabricated memristive cells. The maximum absolute value of the current during the RESET process is predominantly in the range of 1–1.5 μA, while the maximum absolute value of the current during the SET process is approximately 2 μA for the majority of devices.

B. Retention of resistive states

Table S3. The results of a statistical analysis of the retention of 16 resistive states of ZrO_2(Y)-based memristive device.

R	**Average value, Ω**	**Standard deviation, Ω**	**Coefficient of variation, %**
R1	156.1	0.4	0.3
R2	222.2	0.5	0.2
R3	312.0	2.5	0.8
R4	437.2	7.1	1.6
R5	673.9	12.8	1.9
R6	976.6	25.0	2.6
R7	1180.9	21.0	1.8
R8	1565.8	28.9	1.8
R9	1788.4	35.4	2.0
R10	2709.0	126.9	4.7
R11	4846.9	105.1	2.2
R12	5964.1	225.0	3.8
R13	8056.1	212.1	2.6
R14	10770.1	261.1	2.4
R15	12144.7	198.3	1.6
R16	13494.8	288.0	2.1

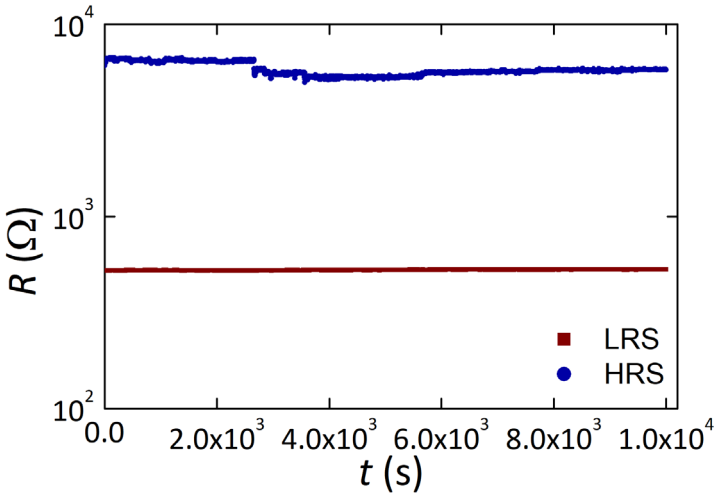


Figure S2. Retention of the extreme resistive states of ZrO_2(Y)-based memristive device.

The analysis of the results of a study of the retention of the extreme resistive states (**Figure S2**) of a memristive device showed that the average values (μ) of the resistance in high resistance state (HRS) and low resistance state (LRS) and its standard deviation (σ), as well as the coefficient of variation ($c = \sigma / \mu$) have the following values: μ_{HRS} = 5808.2 Ω, σ_{HRS} = 429.6 Ω, c_{HRS} = 7.4 %; μ_{LRS} = 526.1 Ω, σ_{LRS} = 2.0 Ω, c_{LRS} = 0.4 %.

C. Potentiation and depression

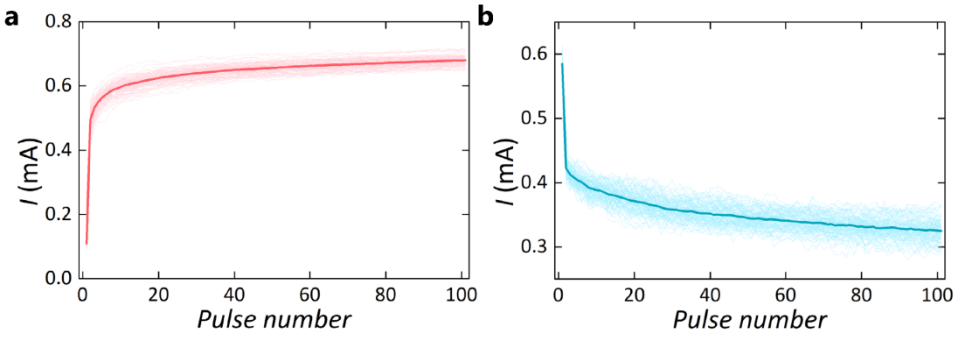


Figure S3. 100 realizations of (a) RESET-potentiation and (b) SET-depression, as well as the corresponding averaged curves.

An assessment of the magnitude of the change in synaptic weight showed that after applying the 2nd pulse of potentiation, the resistive state changes by 1.08±0.04; after applying the 10th pulse of potentiation, 1.22±0.06; and after applying the 100th pulse of potentiation, 1.38±0.08. The value of the standard deviation was used as an error. In the case of depression, these values have the following values: 0.98±0.02, 0.92±0.03, and 0.77±0.04, respectively. The calculated values of changes in synaptic weight represent changes in the resistive state of the memristive device during the implementation of behavioral mechanisms of biological synapses, which are supposed to be the basis of learning and memory, namely paired-pulse facilitation/depression, post-tetanic potentiation/depression, and long-term potentiation/depression, respectively.

D. Transmission electron microscopy data

The elemental distribution maps obtained via energy-dispersive X-ray spectroscopy (EDS) confirmed the elemental composition of the Au/Ta/ZrO_2(Y)/Pt memristor layers (**Figure S4**).

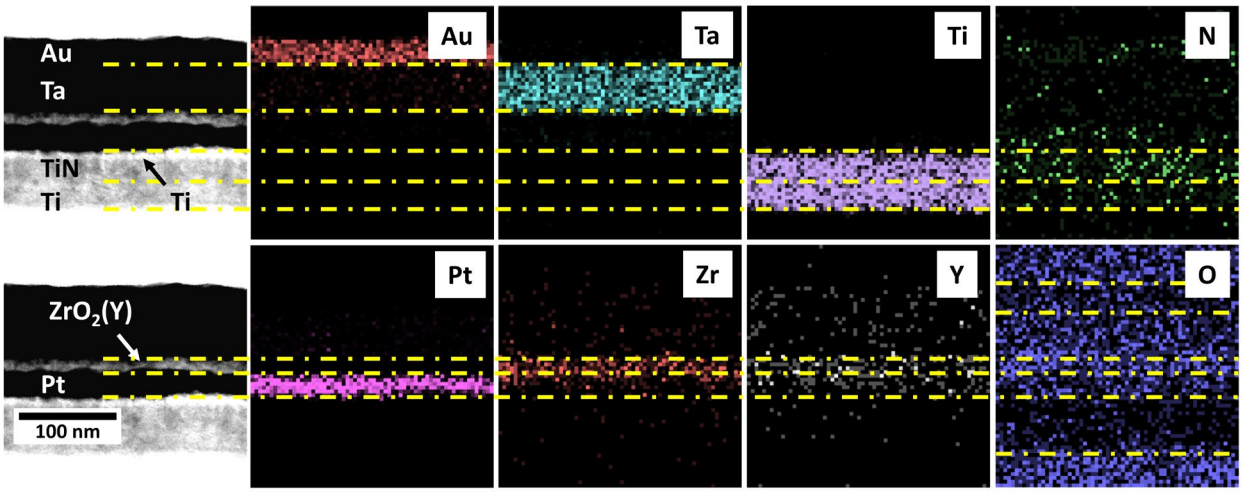


Figure S4. The bright-field scanning transmission electron microscope (TEM) image of the memristor cross-section and the corresponding elemental distribution maps obtained via EDS. All images are the same scale.

EDS mapping revealed oxygen enrichment within the Ta layer (**Figure S4**), consistent with X-ray photoelectron spectroscopy (XPS) data reported for an analogous Ta/ZrO_2(Y) memristor structure in Ref. [111]. Detailed analysis demonstrated that the oxygen concentration near the Ta/ZrO_2(Y) interface exceeds that in the bulk Ta layer. This conclusion is supported by an approximately 1.8-fold decrease in the Ta-M/O-K intensity ratio in the near-interface region, as observed in the integrated EDS spectra (**Figure S5**). To ensure robust comparability, the spectra were normalized in two steps: first, each spectrum was normalized to the integral area under the curve (to eliminate dependence on the signal acquisition area), and then – to the Ta-M line intensity in the spectrum from the bulk of the Ta layer after the first normalization (for clear relative comparison of oxygen content). Comparison with the XPS data [111] suggests that the bright ~ 5 nm-thick band in the Ta layer near ZrO_2(Y) in the TEM images corresponds to a region enriched with TaO_x (**Figure S5**). The observed contrast between Ta and TaO_x arises from the difference in their average atomic numbers (Z). The incorporation of oxygen (Z = 8) into the Ta lattice (Z = 73) reduces the local Z-contrast, which decreases electron scattering in bright-field TEM imaging mode. Consequently, the TaO_x region appears brighter than the bulk Ta layer.

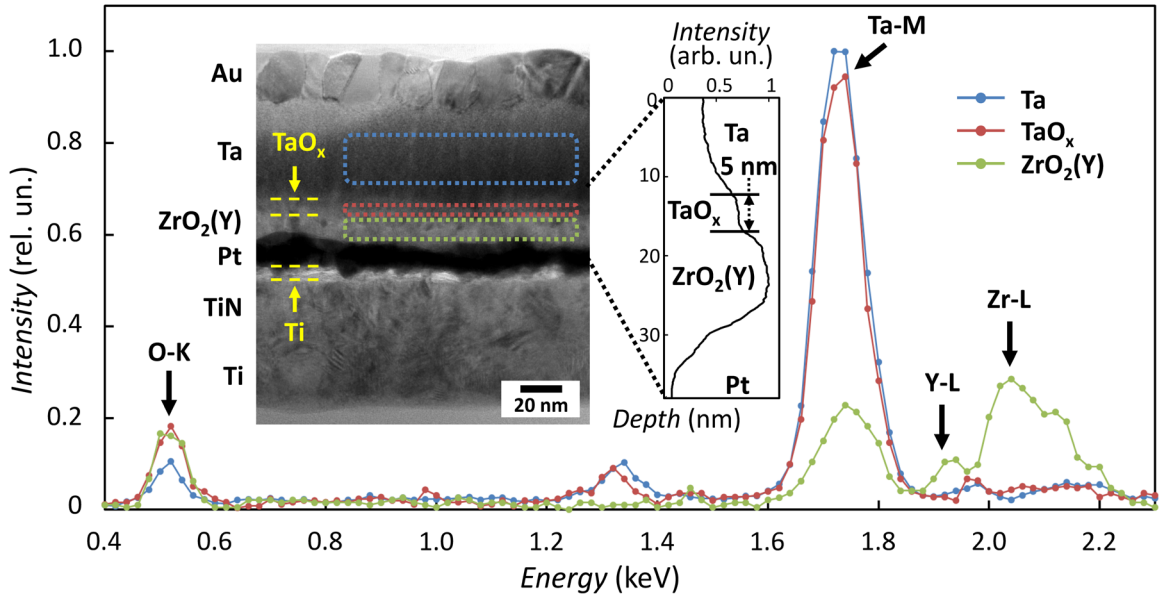


Figure S5. Normalized integrated EDS spectra from selected areas in the TEM image. Insets show the TEM image of the investigated area (left) and the integrated intensity profile from the selected area (right).

The combination of selected-area microdiffraction and sequential layer removal via an ion milling system enabled structural characterization of each memristor layer and the underlying layers (**Figure S6**). The structure of the layers, Au, ZrO_2(Y), Pt, TiN, and Ti (beneath the memristor), is polycrystalline. In contrast, the structure of the Ta is amorphous. The Ti layer located in the memristor has an amorphous matrix with nanocrystalline inclusions. The space group of the grains in the polycrystalline layers (excluding Ti) is $Fm\bar{3}m$ (№ 225, International Tables for Crystallography, Vol. A). The grains of the Ti polycrystal have space group $P6_3/mmc$ (№ 194), indicating the formation of the α-Ti phase. For all materials except ZrO_2(Y) (whose composition was not definitively established), the interplanar distances derived from diffraction patterns match tabulated values within experimental error (**Tables S4, S5**).

Table S4. Interplanar distances (Å): measured (d_{hkl}^{exp}) from selected-area diffraction patterns (**Figure S6**) and calculated (d_{hkl}^{calc}) using tabulated lattice parameters *a* for the corresponding materials. The results are presented for materials belonging to space group $Fm\bar{3}m$.

hkl ($Fm\bar{3}m$)	**Au, *a* = 4.08 Å [112]**		**Pt, *a* = 3.92 Å [112]**		**TiN, *a* = 4.24 Å [113]**		**ZrO_2(Y)**
	d_{hkl}^{calc}	d_{hkl}^{exp}	d_{hkl}^{calc}	d_{hkl}^{exp}	d_{hkl}^{calc}	d_{hkl}^{exp}	d_{hkl}^{exp}
111	2.35	2.35±0.06	2.27	2.27±0.04	2.45	2.44±0.03	2.98±0.07
200	2.04	2.03±0.02	1.96	1.97±0.03	2.12	2.12±0.02	2.56±0.04
220	1.44	1.43±0.01	1.39	1.39±0.02	1.50	1.50±0.01	1.82±0.02
311	1.23	1.23±0.01	1.18	1.19±0.01	1.28	1.28±0.01	1.55±0.02
222	1.18	1.18±0.01	1.13	1.14±0.01	1.22	1.22±0.01	1.49±0.02
400	1.02	1.03±0.01	0.98	0.99±0.01	1.06	1.06±0.01	1.30±0.01
331	0.94	0.94±0.01	0.90	0.90±0.01	0.97	0.97±0.01	1.18±0.01
420	0.91	0.92±0.01	0.88	0.88±0.01	0.95	0.94±0.02	1.15±0.02
422	0.83	0.84±0.01	0.80	0.80±0.01	0.86	0.87±0.01	1.06±0.01
511	0.78	0.79±0.01	0.76	0.76±0.01	0.82	0.82±0.01	0.99±0.01

Table S5. Interplanar distances (Å) for α-Ti (space group: $P6_3/mmc$): measured (d_{hkl}^{exp}) from the selected-area diffraction pattern (**Figure S6**) and calculated (d_{hkl}^{calc}) using tabulated lattice parameters *a* and *c*.

hkl ($P6_3/mmc$)	**α-Ti, *a* = 2.95 Å, *c* = 4.68 Å [114]**		**hkl ($P6_3/mmc$)**	**α-Ti (continuation)**	
	d_{hkl}^{calc}	d_{hkl}^{exp}		d_{hkl}^{calc}	d_{hkl}^{exp}
100	2.56	2.57±0.04	**200**	1.28	1.29±0.01
002	2.34	2.36±0.03	**112**	1.25	1.25±0.02
101	2.24	2.25±0.03	**201**	1.23	1.23±0.01
110	1.48	1.49±0.01	**004**	1.17	1.18±0.01
103	1.33	1.32±0.01	**202**	1.12	1.13±0.02

Using the cubic lattice formula $a_{hkl} = d_{hkl}\sqrt{h^2+k^2+l^2}$, the lattice parameter of ZrO_2(Y) was calculated as (5.15 ± 0.02) Å. Note that this parameter is the average value over the analyzed region.

Diffraction data were confirmed by high-resolution TEM (HRTEM) and Fourier transform analysis (FT) (**Figure S7**).

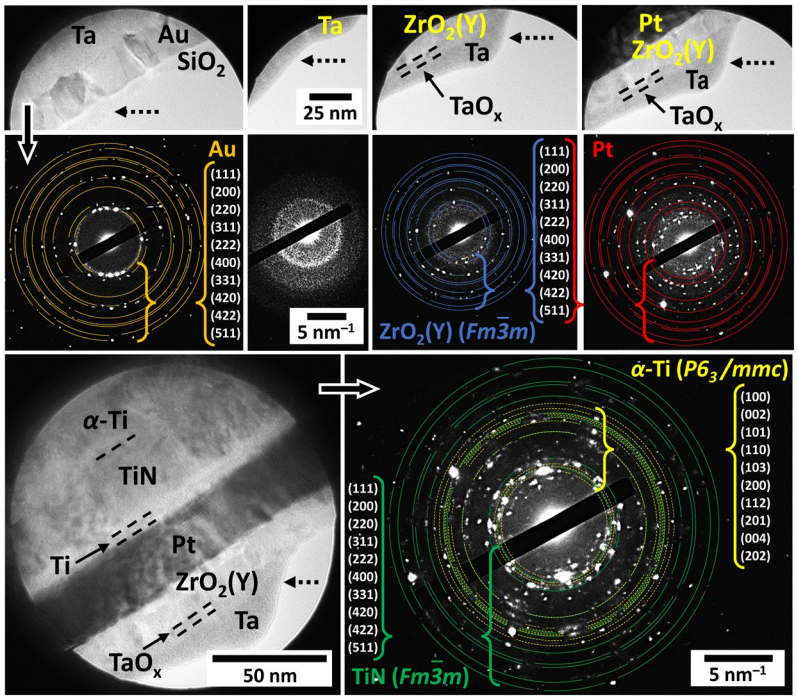


Figure S6. Selected-area diffraction patterns (SADPs) of the memristor cross-section. The scales for all TEM images are identical, as are the scales for all SADPs, except for the TEM image and SADP from the entire structure without Au – the two lower images. The dotted arrow indicates the perforation edge.

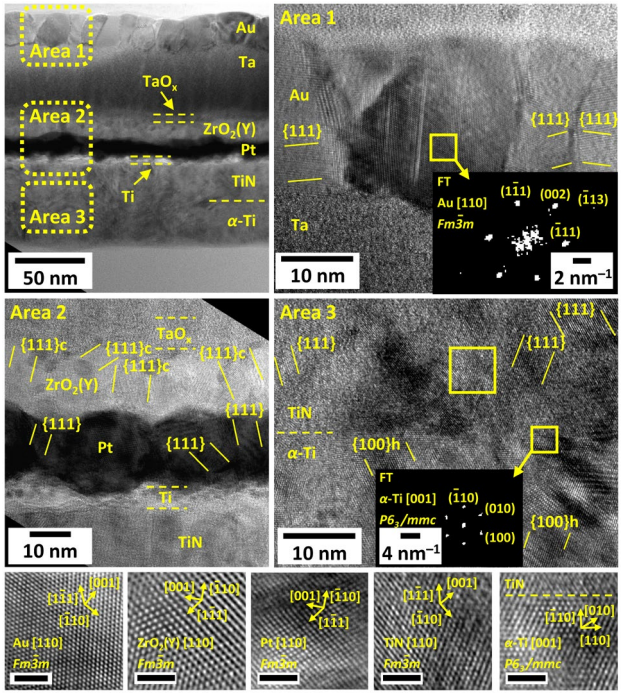


Figure S7. High-resolution TEM (HRTEM) images of the memristor cross-section within an integrated circuit. FT – Fourier transform. In the HRTEM images of individual grains, the scale bar represents 2 nm. Miller indices {hkl} in curly brackets indicate the family of planes marked by the lines. Miller indices {hkl} in curly brackets without a symbol or with the symbol "c" refer to the cubic lattice, while those with the symbol "h" refer to the hexagonal lattice.

E. Neural network simulation

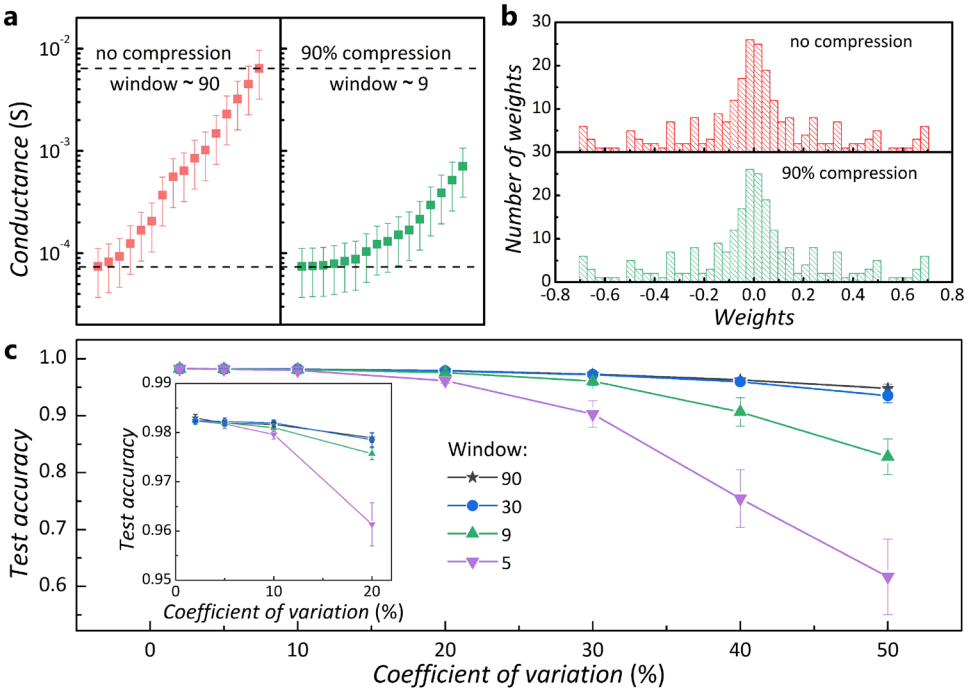


Figure S8. a) Initial experimental 16 states and an example of their compression. b) Histogram of the possible memristive scaled weights, calculated as all possible differences between 2 states (experimental/compressed). c) Accuracy of the Modified National Institute of Standards and Technology test dataset classification depending on the coefficient of variation of the resistive states and the resistive window of the memristor (experimental/compressed).